Wave: Jurnal Ilmiah Teknologi Maritim Volume 14 Nomor 1, Juli 2020: Hal: 1-8

THE SIMULATION OF SKEG EFFECT TO BARGE RESISTANCE USING CFD-RANS OPENFOAM

Abrari Noor Hasmi[1] dan Samsu Dlukha Nurcholik[2]

[1]Dosen Institut Teknologi Kalimantan, Balikpapan

Email: abrari@lecturer.itk.ac.id

Diterima: 16 Januari 2020; Direvisi: 02 Maret 2020; Disetujui: 19 Maret 2020

Abstrak

Makalah ini membahas pengaruh beberapa macam variasi bentuk *skeg* terhadap tekanan, kecepatan fluida dan hambatan total kapal. Ada tiga variasi bentuk *skeg*: kapal tongkang tanpa *skeg*, kapal tongkang dengan *skeg* tanpa defleksi dan kapal tongkang dengan skeg berdefleksi. Kapal dijalankan dengan kecepatan 3–9 knot. Simulasi dilakukan dengan beberapa kecepatan antara 3–9 knot. Simulasi dijalankan menggunakan program CFD RANS sumber terbuka OpenFOAM. Simulasi menunjukkan bahwa *skeg* mengakibatkan kenaikan hambatan kapal. *Skeg* dengan defleksi memiliki amplifikasi hambatan hampir 50%, jauh lebih besar dibandingkan 5% amplifikasi hambatan pada *skeg* tanpa defleksi.

Kata kunci: hambatan, komputasi, dinamika, fluida, *skeg*, OpenFOAM

Abstract

This paper discusses the significance of different types of skegs in a barge toward the pressure, fluid velocity and the ship's total resistance. There are three kinds of skeg configurations: barge without skegs, skegs without deflection and skegs with deflection. The barge was towed with forward speed were ranging across 3–9 knots. The simulations were conducted using an open-source RANS (Reynold Averaged Numerical Simulation) CFD code Open-FOAM. The simulations show that the skegs raise the barge's resistance. The skegs with deflection attenuate the resistance approximately 50%, this is far larger compared to 5% resistance amplification in skegs without deflection.

Keywords: *resistance, computational, fluid, dynamics, skeg, OpenFoam*

INTRODUCTION

A barge is one of the primary vehicles widely used in Kalimantan to transport bulk goods such as coal. The convenient to use barge stems from the fact that it can reach the main rivers whose water depth is shallow.

A skeg is a modification attached to the ship stern. An experiment using box type and hexagon type barge showed that the measured slew angle from around 30° in the bare stern to less than 1% by skegs attachment (Im et al., 2015). However, researchers in (Jang-Ho et al., 2011) showed that the skeg could augment 30% toward the barge resistance. In this regard, considering the demand to reduce ship emissions, which requires the reduction of ship resistance, one has to choose the best skeg design to minimize the additional barge's resistance.

The model test has been a reliable means to

determine the resistance of a ship in various complex conditions. Nevertheless, as the experiment requires a significant amount of cost and has to be conducted at sophisticated towing tank facilities, thus an alternative approach, namely numerical simulation has widely acknowledged as a reliable tool for predicting the ship resistance. Furthermore, as pointed out in (Niklas and Pruszko, 2019) the extrapolation of the model scale measurement to full-scale result may be inaccurate due to various assumptions in the approach. Some of them are the form factor and friction line, even though the model test is still used to validate the result of computer programs.

In order to compute the ship resistance, there are several methods available in the literature. A common technique is by using predefined regression formulas, which are based on the best experimental fit over a systematic and extensive set of data. The formula used is dependent on the ship's shape and its main dimension, and then later corrected to take ship's appendages such as bulbous bow, fin or skeg into account. An example of this method was proposed in (Holtrop, 1984) based on systematic experimental campaigns on extensive hull shapes. This technique could give an initial estimate of resistance, however, should be employed with cautious of its caveat, especially if the ship's hull is rather uncommon (Niklas and Pruszko, 2019), such as the unusual shape of the bow, skegs, etc. One method that is more generic is by explicitly simulate the flow at the ship's vicinity through computational methods. This method can cover more general ship's geometries and becomes feasible due to the advancement of both computation hardware and algorithm.

At least there are two main computational methods which are widely known: the potential method which utilizes three dimensional Rankine's panel to discretize the ship's hull and water's surface (Zhang et al., 2016). In this method, the fluid is usually assumed ideal; in other words, the viscosity of the fluid, the effect of the boundary layer, and the turbulence are ignored. The second method is the viscous computation which solves some variants of the Navier-Stokes equation, most often by using Reynolds Average Navier Stokes (RANS) equation (Priyanto et al., 2015; Chen et al., 2016). In this method, the field is discretized, namely by using finite volume method. The flow is divided into mean and fluctuation. Then additional equations are introduced to represent the turbulence.

Several researchers have utilized the computational fluid dynamics with various codes for investigating the impact of skeg on vessels' resistance. A study was conducted to compare the efficiencies of twin skegs on an LNG ship using SHIPFLOW. The calculation for twin skegs was compared with single skeg and concluded that the twin skeg could achieve up to 13% reduction in resistance (Kim et al., 2014). Likewise, research in (Priyanto et al., 2015) calculated the resistance of twin skeg container vessel with several sets of mesh resolution employing commercial code ANSYS CFX.

In our research, we endeavoured to investigate the effect of several skeg angles on the barge resistance using OpenFOAM. OpenFOAM is an open-source and free computational fluid dynamics solver based on C++ which capable of solving numerous fluid problems. The code has been widely used and validated to calculate problems in marine engineering, among them are resistance calculation of a catamaran (Bustos and Alvarado, 2017) and the calculation of added resistance of a cruise ship (Moctar et al., 2017).

METHODS

Mathematical Methods

This section describes a brief explanation of the principles behind the computational fluid dynamics implemented in OpenFOAM. The interested reader can refer to (Holzmann, 2017) for more detailed elaboration about the derivations of the equations in OpenFOAM and consult (Moukalled et al., 2016) which presents a more elaborate explanation of finite volume method and the turbulence modelling in OpenFOAM.

The computation fluid dynamics for ship resistance mainly assumes that the fluid is viscous but incompressible. The incompressibility assumption is justified since the water has a very large density and the temperature does not change very much in the waterline. The main physics governing the fluids are the incompressible Navier Stokes equation:

$$\nabla . \rho U = 0 \tag{1}$$

$$\frac{\partial}{\partial_t} \rho U + \nabla(\rho U \otimes U) = -\nabla \sigma + \rho g \tag{2}$$

The equation (1) is the mass conservation, which tells that the net sum of mass in an infinitesimal volume should be zero. The equation (2) is the momentum equation, which describes all the exchange

of momentum acting on the volume. Here $U = (U_x, U_y, U_z)$ are the fluid velocity at (x, y, z) directions, ρ is the fluid density, g is the gravitational acceleration, while σ is Cauchy stress tensor (Holzmann, 2017). The notation $\otimes$ denotes the outer product of two vectors.

The turbulence usually has a smaller scale compared to the main flow. In general, explicitly resolving all the smallest turbulence requires a very small time step and spatial discretization, which result in a resource-intensive task. To circumvent this situation, the turbulence is not explicitly resolved but modelled by dividing the velocity into its mean and fluctuation part, which has zero mean over a period. For instance, fluid velocity could be written as:

$$U = \overline{U} + U' \tag{3}$$

With the bar denotes the mean part of the flow, while tilde signifies the fluctuation part. The fluctuation part satisfies the following time averaging condition:

$$\lim_{T\to\infty} \frac{1}{T}\int_t^{t+T} \emptyset'(t,x) = 0 \tag{4}$$

The substitution of the approximation to equations (1) and (2) then taking the time average yield the Reynold Time Average Navier-Stokes equation:

$$\frac{\partial \rho}{\partial t} + \nabla(\rho\overline{U}) = 0 \tag{5}$$

$$\frac{\partial}{\partial_t}\rho\overline{U} + \nabla(\rho\overline{U}\otimes\overline{U}) = -\nabla\overline{\sigma} + \rho g - \nabla(\rho U'\otimes U') \tag{6}$$

Comparing this equation with the original equation, overall both equations have the same form, except additional last term in the equation(6). This term, usually called as Reynold-Stress, is unknown. Thus adding the unknown in the equations into five while there are only four equations provided. Hence, additional equations are required to solve the Navier-Stokes equations. Consequently, the Reynold-Stress will be modelled, and the turbulence model used in the simulation is the $k-\omega$ SST model (Menter, 1994). The model combines k - ϵ and $k-\omega$ formulation, together with improvement in turbulent shear stress.

The volume of fluid method captures the air and water interface. Briefly stated, at each control volume, the volume fraction is computed, with 0 denotes air area, 1 indicates the cell is filled with water and value between 0 and 1 to models the interface. Let α means the volume fraction. Then the density is stated as:

$$\rho = \alpha\rho_l + (1-\alpha)\rho_g \tag{7}$$

where ρ_l is the water density while ρ_g denotes the air density. To preserve the sharp interface, compression flux was introduced at the free surface.

Practically, the OpenFOAM solver called *interfoam* was employed as an implementation of the VoF approach. The solver supports solving a problem involving dynamic meshes. The time-stepping procedure was based on the PIMPLE method which is a combination of SIMPLE (Semi Implicit Method Of Pressure Linked Equations) method and PISO (Pressure Implicit with Splitting of Operators) (Holzmann, 2017). The SIMPLE method is an algorithm to solve the steady-state part of the solution, while PISO solves the transient part. By combing those two methods, PIMPLE could use a higher Courant number. Reference (Deshpande et al., 2012) presented the details of the algorithm in the *interfoam.*

Together with the turbulence model, the Navier Stokes equations are discretized using the finite volume method and volume of fluid. The details of the method are not presented here, readers are encouraged to refer more elaborate introduction to the finite volume method implemented in OpenFOAM (Moukalled et al., 2016).

Ship Geometry

In this research, the ship used is a barge designed by PT Asia Aditama Shipyard, with the main dimensions given in Table 1, and while the line plan is shown in Figure 1.

Table 1. Barge main particulars

LOA	91.44 m
Breadth	24.84 m
Depth	5.486 m
WSA	2763 m^2
Volume	8378 m^3

The barge's line plan was drawn in a CAD program Maxsurf modeller. The line plan was exported into a .STL extension, which is readable by Open-FOAM. In CAD preparation, the ship's should form a closed surface.

A skeg is an appendage attached at the stern area. The attachment of skegs is known to be able to improve the course stability, primarily by reducing the yaw motion. The mechanism behind the improved yaw

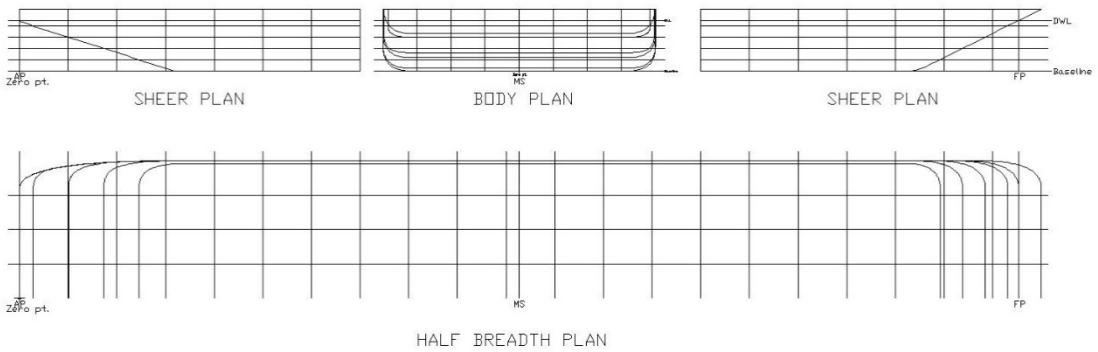

Figure 1. Barge's line plan

stability is by smoothing the flow from the hull, thus reducing the turbulence at the stern. Skeg has been applied to various types of vessel, either self-propelled or towed. In the self-propelled ship, the skeg primarily placed in front of propeller such that the water flows into the propeller smoothly. Authors in (Kim et al., 2014) optimized the hull shape for twin skeg LNG vessel. Furthermore, researchers in (Kwon et al., 2015) compared the effectiveness of single and twin skegs configuration for towed FPSO ship in reducing the yaw motion.

In the research, we are concerned with the towed barge, which usually cruises in rivers in Kalimantan. We primarily observed the impact of the barge during a straight course and mainly wanted to examine how much resistance rises as those two skegs configuration were installed. The course stability will be the subject of our follow up studies.

The simulations were conducted with three skegs variation: Barge without a skeg, barge with 180 degrees skegs and barge with 150 degrees skegs. Figure 2 shows the skeg configuration for 180° and 150°. The skegs definitely raise the barge's wetted surface area. The wetted surfaces area is 2328.41 m^2 for barge without a skeg, 2437.6 m^2 for the barge with 180° skegs and 2442.53 m^2 for the barge with 150° skegs. In short, the 180 and 150 degrees skegs contribute to approximately 4.6% and 4.9% respectively additional wetted surface area compared to the barge without a skeg.

The barge variation with a skeg angle of 180° has the following coordinate position; the front of the skeg is on the offset coordinate of 9 meters from the centerline, and in the longitudinal coordinate position of 12,026 meters from the zero coordinate, which is right at the rear end of the ship. While the rear of the skeg is the same offset coordinate which is 9 meters from the centerline, and in the longitudinal coordinate position of 0.1 meters from the very back of the ship. In this configuration, there is no coordinate deflection in the skeg.

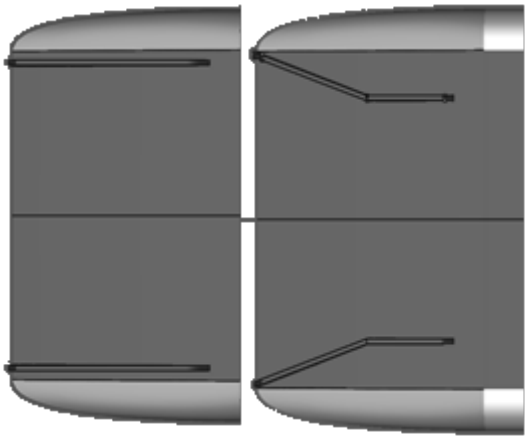

Figure 2. Skeg configuration: 180 degrees (left), 150 degrees (right)

Whereas, on barge variations with skeg 150 angles having the skeg coordinate position as follows: the front of the skeg has offset coordinate 7 meters from the centerline, and in the longitudinal coordinate position of 12,026 meters from zero coordinate which is right behind the ship. Then the position of the deflection curve in the skeg is at the offset coordinate of 7 meters, and the longitudinal coordinate position is 6,855 meters from the very back of the ship. The rear part of the skeg has an offset coordinate of 9.5 meters from the centerline, and in the longitudinal position coordinates of 0.1 meters from the very back of the ship.

The barge's line plan was drawn in a CAD program Maxsurf modeler. The line plan was exported into .STL extension which is readable by Open-FOAM. In CAD preparation, the ships should form a closed surface.

Simulation Setups

The simulation was performed in the following setting: The water depth was 19.5 meters, the longitudinal computational domain was more than three times the ship's length, while the transverse computational domain was 2.5 of ship's half breadth. The distance from upstream and the ship's bow is approximately 1.2 Lpp while the downstream boundary located about 0.87 Lpp from the ship's stern. Due to symmetry, only transverse half of the geometry was simulated. Notice that the simulations were performed in full-scale condition. The computational domain is illustrated in Figure 3.

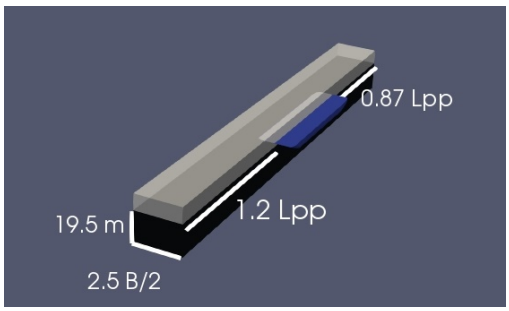

Figure 1 Computational domain

The mesh was designed in two main steps: The first step is the set-up of background mesh. At this stage, the non-overlapping hexagonal shape volumes divided the computational domain. The size of the hexagon varied along with the domain. The cells close to the ship have a smaller volume. This action is aimed to sufficiently resolve the essential part of simulation by discretizing region in which the flow change most. The transition from dense to coarse mesh size transition should be gradual to ensure smoothness of the solution. The background meshes had hexagonal shapes. The second step is to snap the mesh conforming the hull shape. The built-in OpenFOAM utility, called snappy-HexMesh, was utilized to transform the mesh in the vessel's vicinity into an irregular mesh. The snappy-HexMesh snap the mesh encircling the barge hull by iteratively splitting, and morph meshes adjacent to the surface. The simulations used approximately 1 million cells.

The simulations were performed with different velocities, ranging from 3 knots to 9 knots which are typical for barge maneuvering. The simulations were performed in a calm water condition with water density 998.8 (freshwater). Thus, the additional resistance due to wave and wind are ignored. The simulations were executed using the two-phase unsteady interfoam solver with dynamic meshing in the OpenFOAM. All the simulations were done in simulation time correspond to 80s.

During the simulation, the values of hull pressure components were recorded at each time step. The pressure components consist of integrated pressure along with the three translation and three rotation axis; each direction consists of normal pressure component and viscous component. In term of the resistance components, the normal pressure usually called wave-making resistance, while the viscous part is the friction resistance.

RESULT AND DISCUSSION

Visualization of the dynamic pressure contour on the barges hulls at 7 knots can be observed in Figure 4.

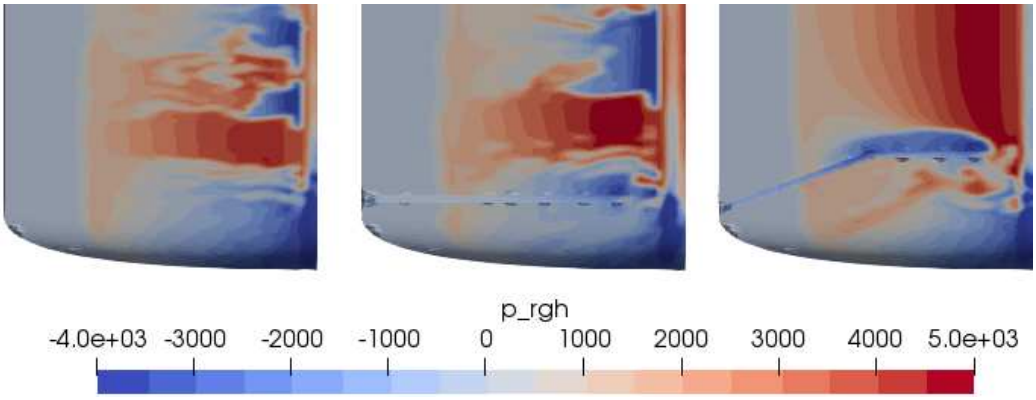

Figure 4. Dynamic pressure at barge's stern at 50s : without skeg (left), 180° skeg (middle), 150° skeg (right)

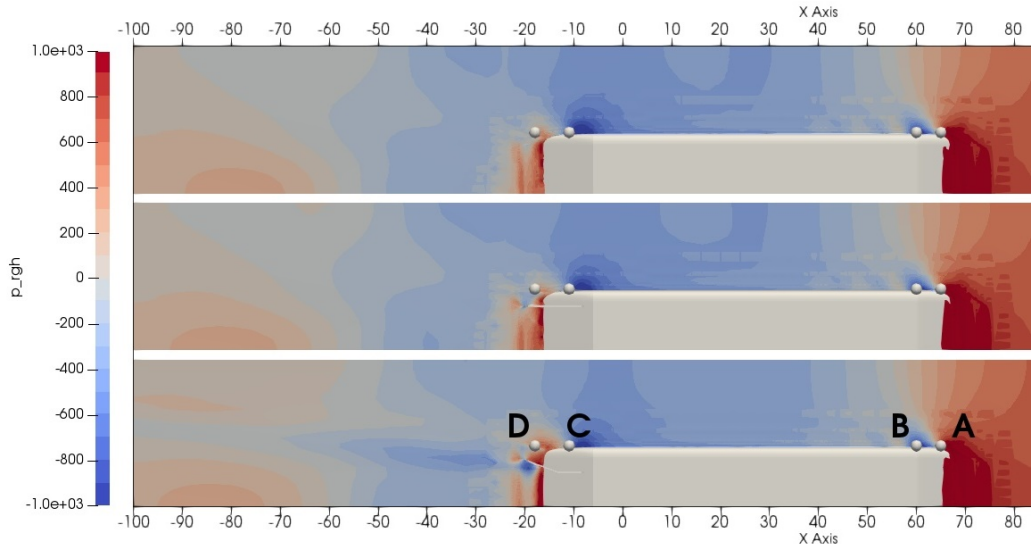

Figure 5. Pressure contour at free surface: without skeg (top), 180° skeg (middle), 150° skeg (bottom)

The dynamic pressure is defined as the remainder of normal pressure after subtracted with static pressure at a particular depth, namely the barge's draft. The figure shows the pressure contour observed from the bottom at 50 seconds. The color legend scale is ranging from -4000 N/m^2 until 5000 N/m^2. The pale blue colour near the transom marks area above the waterline.

From the figure, it is evident that the pressure contour in barge without skeg and with 180° skegs seems alike, in contrast with the barge with 150° skegs, which has a very different pattern. The high pressure along the transverse area in between 150° skeg does not present in the rest of geometries, which possess changing pattern between low and high pressure in the transverse direction. Moreover, the area outward of 150° skeg has some area coloured with dark red marking that the pressure is still high in that area. The high local pressure because the skegs obstruct the water flow. Thus, the water flow from the bow is turned following the skeg shape. The other geometries also have areas with dark red colour near lateral sides. However, the areas are both smaller and less dark red compared with the ones that belong 150 skegs.

Figure 5 depicts the dynamic pressure contours at the free surface 50 seconds after the beginning of the simulation for three geometries. The pressure contours near the bow area have a similar pattern. In all cases, the noticeable high pressure near the bow in all cases is due to bow's bulk shape, which results in a vast amount of water need to be displaced through the sides of the barges. At both sidewalls, a wave-like pattern, which is observed with high pressure (red colour), indicates crest and area with low-pressure shows wave's through.

The figure reveals that there is a noticeable wake behind the skeg with deflection. This wake induces higher wave-making resistance, which consequently raises the barge's resistance.

The free surface elevation along $y = -12.45$ at $t = 50$ s is plotted in Figure 6. This location is next to the sides of the barges. We annotated the main features of the graph. The point A is located just in front of barge's bow, where the water displaced by the barge's bow is accumulated and result at very high elevation at this point. This displaced water propagated along the sides of the barges generated a wave-like pattern with the first through observed at point B. Points C is the suction point adjacent to the transom joints, while point D is located just behind the stern. The figure supports our previous assertion that the amplitude of wake generated by deflected barge is higher, thus implying that the wave-making resistance is higher in the barge with deflection.

The most relevant quantity in our discussion is the ship's total resistance. The resistance has a direct contribution to the power efficiency of the ship. A smaller resistance yield lower power, which leads to higher fuel efficiency. Thus, it is important to observe at the barge's resistance.

The total resistance is defined as the time average of exerted resistance. As only half of the barge was simulated, we should multiply the calculation of the

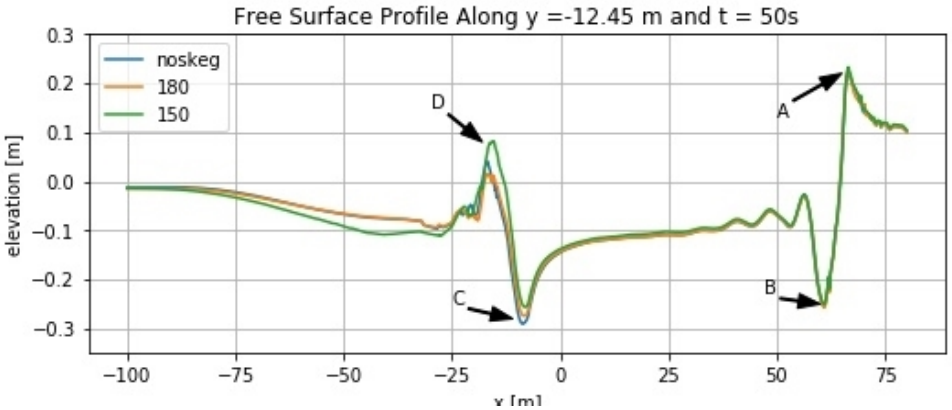

Figure 6. The free surface profile at sides of the barge at 50s

half body barge's resistance by two, in order to get the full bodies resistance. During the resistance computation, pressure during initial time is ignored, as they correspond to the unphysical situation where the barge was suddenly accelerated from rest to the intended advance velocity.

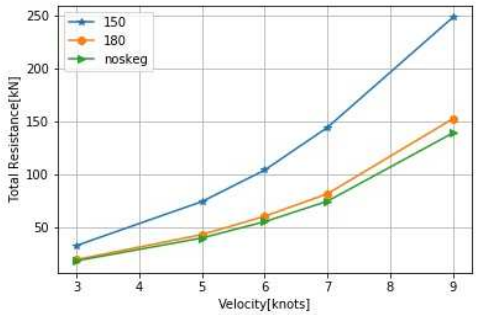

Figure 7. Barge's total resistance

The total (full body) resistance is plotted in Figure 7, while its numerical values are presented in Table 2. From the figure, it is evident that the barge without skegs always has the lowest resistance. The skeg, in general, raises the resistance, this could be attributed to the additional underwater surface area. However, the resistance amplification is different between two skegs configurations. The skeg with deflection has the highest resistance, up to 50% resistance amplification compared to barge without skegs. Thus, this skeg configuration is unfavourable as the rise in resistance is quite significant. The skeg without deflection shows a slight increase in the resistance, approximately 5% compared to barge without the skeg.

Comparing the main source of the rise in resistance, the surface area and consequently, the frictional resistance is the main factor behind the amplification of 180° skeg. However, regarding 150° skeg, the rise in surface area is insignificant compared to the increase of resistance. Thus other factors might contribute to the resistance surge, namely the wave-making resistance as the deflected skeg block the downstream flow.

Table 1. Barge's total resistance

V (knot)	Total Resistance (kN)		
	Without Skeg	180°	150°
3	18.060	19.131	32.455
5	39.540	42.736	73.933
6	54.909	59.385	103.648
7	74.222	81.207	143.830
9	138.611	151.996	247.784

Despite this finding, the main reason behind the attachment of a barge in the stern is to improve the directional stability of the barge during maneuvering (Im et al., 2015; Lee et al., 2017). Thus, although the barge without skeg has smaller resistance compared to the barge with 180° skeg, the barge without skeg may suffer stability problem during maneuvering. This assertion should be further verified for instance, by using another CFD simulation.

CONCLUSION

This paper has demonstrated the consequences of different skeg configuration for the barge resistance utilizing CFD simulations using Open-FOAM. The skeg, especially the one with deflection, induce higher pressure at the stern's lateral sides. Higher

ship-generated waves behind the barges are observed in the case of the deflected barge.

The simulations with different skegs configurations show that, in general, the skeg amplifies the barge resistance. However, the amplification depends on the geometry of the skeg, the skeg with deflection attenuate the resistance higher than the skeg without deflection.

ACKNOWLEDGMENT

The authors would thank anonymous reviewers for their contribution to improve the manuscript.

REFERENCES

Bustos, D. S. H. & Alvarado, R. J. P. (2017). Numerical Hull Resistance Calculation of a Catamarán using OpenFOAM. *Ship Science & Technology*, Vol. 11(21): 29-39.

Chen, J., Wei, J. & Jiang, W. (2016). Optimization of a Twin-skeg Container Vessel by Parametric Design and CFD Simulations. *International Journal of Naval Architecture and Ocean Engineering*, Vol. 8(5): 466-474.

Deshpande, S. S., Anumolu, L. & Trujillo, M. F. (2012). Evaluating the Performance of the Two-Phase Flow Solver InterFoam. *Computational Science & Discovery*, Vol. 5: 1-36.

Holtrop, J. (1984). A Statistical Re-analysis of Resistance and Propulsion Data. *International Shipbuilding Progress*, Vol. 89(363): 272-276.

Holzmann, T. (2017). *Mathematics, Numerics, Derivations and OpenFOAM (R)*. Leoben: Holzmann CFD.

Im, N. K., Lee, S. M. & Lee, C. K. (2015). The Influence of Skegs on Course Stability of a Barge with a Different Configuration. *Ocean Engineering*, Vol. 97: 165–174.

Jang-Ho, C. Moon-Chan, K., Ho-Hwan, C. & In-Rok, D. (2011). Correlation Study on Course Keeping Stability of Barges according to Variations in Dimensions and Hull Coefficient. *Journal of Ocean Engineering and Technology*, Vol. 25(5): 27-32.

Kim, K., Tillig, F., Bathfield, N. & Liljenberg, H. (2014). Hydrodynamic Optimization of Twin-Skeg LNG Ships by CFD and Model Testing. *International Journal of Naval Architecture and Ocean Engineering*, Vol. 6(2): 392-405.

Kwon, C. S., Kwon, O. J., Lee, S. W. & Kim, H. T. (2015). Prediction of Course Stability of Towed Offshore Structures by Computational Fluid Dynamics. *International Journal of Offshore and Polar Engineering*, Vol. 25(02): 97–103.

Lee, S. M., Luong, T. N. & Im, N. K. (2017). The Effects of Skegs and Length of Towline on Trajectory Characteristics of Barge. *Journal of the Korean Society of Marine Environment and Safety*, Vol. 23(4):385-392.

Menter, F. R. (1994). Two-Equation Eddy-Viscosity Turbulence Models for Engineering Applications. *AIAA Journal*, Vol. 32(8): 1598–1605.

Moctar, O. E., Sigmund, S., Ley, J. & Schellin, T. E. (2017). Numerical and Experimental Analysis of Added Resistance of Ships in Waves. *Journal of Offshore Mechanics and Arctic Engineering,* Vol. 139(1): 11301–11309.

Moukalled, F., Mangani, L. & Darwish, M. (2016). *The Finite Volume Method in Computational Fluid Dynamics: An Advanced Introduction with OpenFOAM® and Matlab*. New York: Springer.

Niklas, K. & Pruszko, H. (2019). Full-scale CFD Simulations for the Determination of Ship Resistance as a Rational, Alternative Method to Towing Tank Experiments. *Ocean Engineering*, Vol. 190: 106435.

Priyanto, A., Ahmed, Y. M., Zulhazazi & Sunarsih. (2015). Numerical Simulation for Hydrodynamic Characteristics of Twin Skeg Container Vessel. *International Journal of Modeling and Optimization*, Vol. 5(4): 277–280.

Zhang, X., Gu, X., Ma, N. & Mao W. (2016). Application of a Rankine Source Method in Seeking for Optimum Trim of a Container Ship with Lowest Wave-Making Resistance. *Proceedings of the 26th International Ocean and Polar Engineering Conference*, 535-542.